Bovine Holo-lactoferrin inhibits migration and invasion in breast cancer cells

Ninive Rodriguez-Ochoa
Centro de Investigacion y de Estudios Avanzados del IPN: Centro de Investigacion y de Estudios Avanzados del Instituto Politecnico Nacional

Pedro Cortes-Reynosa
Centro de Investigacion y de Estudios Avanzados del IPN: Centro de Investigacion y de Estudios Avanzados del Instituto Politecnico Nacional

Karem Rodriguez-Rojas
Centro de Investigacion y de Estudios Avanzados del IPN: Centro de Investigacion y de Estudios Avanzados del Instituto Politecnico Nacional

Mireya de la Garza
Centro de Investigacion y de Estudios Avanzados del IPN: Centro de Investigacion y de Estudios Avanzados del Instituto Politecnico Nacional

Eduardo Perez Salazar (eduardo.perez@cinvestav.mx)
Centro de Investigacion y de Estudios Avanzados del IPN: Centro de Investigacion y de Estudios Avanzados del Instituto Politecnico Nacional https://orcid.org/0000-0002-3041-7902

Research Article

Keywords: Breast cancer, Lactoferrin, Invasion, Migration, FAK, E-cadherin

Posted Date: April 15th, 2022

DOI: https://doi.org/10.21203/rs.3.rs-1531335/v1

Abstract

Purpose Breast cancer is the most common malignancy in developed countries and the leading cause of deaths in women worldwide. Lactoferrin (Lf) is a non-haem iron-binding glycoprotein constituted for a single polypeptide chain folded into two symmetrical lobes that bind Fe^{2+} or Fe^{3+} and it has the ability to reversibly bind Fe^{3+} and then Lf is present free of Fe^{3+} (Apo-Lf) or associated with Fe^{3+} (Holo-Lf) with a different three-dimensional conformation. However, the role of bovine Apo-Lf (Apo-BLf) and/or Holo-BLf in the inhibition of migration/invasion induced by linoleic acid (LA) and fetal bovine serum (FBS), and in the expression of mesenchymal and epithelial proteins in breast cancer cells remains to be clarified.

Methods and results Based on scratch wound assays results demonstrate that BLf does not induce migration, but Holo-BLf and Apo-BLf differentially inhibit the migration induced by fetal bovine serum (FBS) and linoleic acid (LA) in MDA-MB-231 breast cancer cells. Moreover, based on western blot, invasion, zymography and immunofluorescence confocal microscopy, findings demonstrate that Holo-BLf partly inhibit the invasion, FAK phosphorylation at tyrosine (Tyr)-397, secretion of MMP-2 and MMP-9, and an increase in the number and size of focal adhesions induced by FBS in MDA-MB-231 cells. Moreover, Holo-BLf induced inhibition of vimentin expression in MDA-MB-231 and MCF-7 breast cancer cells.

Conclusion Findings demonstrate that Holo-BLf inhibit cell processes involved with the invasion process in breast cancer cells.

Introduction

Breast cancer is the most common malignancy in developed countries and the leading cause of death in women worldwide [1]. The higher incidence rates of breast cancer are common in high-income countries, but recently it has been reported a rising in low- to middle-income countries, due to a variety of factors including aging and lifestyle changes, such as dietetic factors [2–4].

Lactoferrin (Lf) is a non-haem iron-binding glycoprotein with high homology among species that transport iron in blood serum, and is produced by mucosal epithelial cells in various mammalian species, such as humans, cows, goats, horses and some rodents [5]. The Lf glycoprotein is present in mucosal secretions and body fluids including saliva, tears, vaginal fluids, semen, blood plasma, amniotic fluid and is abundant in milk and colostrum [6, 7]. Lf is an 80 kDa glycosylated protein constituted for a single polypeptide chain folded into two symmetrical lobes, connected by a hinge region constituted for regions of α-helix. Lobes of Lf bind Fe^{2+} or Fe^{3+} ions but can also bind Cu^{2+}, Zn^{2+}, and Mn^{2+} ions, however Lf has the ability to reversibly bind Fe^{3+} and then Lf is present free of Fe^{3+} (Apo-Lf) or associated with Fe^{3+} (Holo-Lf) with a different three-dimensional conformation depending on its binding to Fe^{3+} [5, 8]. Lf plays important roles in the regulation of iron absorption and the modulation of immune system, however, it has been involved in antimicrobial activity against a broad spectrum of bacteria, fungi, yeast, virus and parasites, as well as with anti-inflammatory and enzymatic functions [9–12].

Lf presents also anticarcinogenic properties because it has preventive effects against gastrointestinal cancers, such as cancer of colon, stomach, liver and pancreas. Moreover, Lf inhibits proliferation and Akt activation in SGC-7901 stomach cancer cells [13–15]. Moreover, bovine Lf (BLf) from milk decreases viability and proliferation, and increase apoptosis in HS578T and T47D breast cancer cells, whereas human Lf induces arrest at G1 to S transition of cell cycle, inhibit Cdk2 kinase activity, hypophosphorylation of Rb and decrease protein levels of Cdk2 and cyclin E in MDA-MB-231 breast cancer cells [16, 17]. However the role of Apo-BLf and Holo-BLf in cell migration and invasion of breast cancer cells remains to be studied.

In this study, we demonstrate that Holo-BLf and Apo-BLf differentially inhibit the migration induced by fetal bovine serum (FBS) and linoleic acid (LA) in MDA-MB-231 breast cancer cells. Holo-Lf partly inhibit the invasion, FAK phosphorylation at tyrosine (Tyr)-397, secretion of MMP-2 and MMP-9, and an increase in the number and size of focal adhesions induced by FBS in MDA-MB-231 cells. Moreover, Holo-BLf induced inhibition of vimentin expression in MDA-MB-231 and MCF-7 breast cancer cells.

Materials And Methods

Materials

Apo-BLf with a purity of 97% was from NutriScience Innovations, LCC (Connecticut, USA). Apo-BLf was saturated with iron to obtain Holo-BLf according to a method described previously [18]; iron in Holo-BLf was 93% and it was quantified by an enzymatic automated method (MicroTech Laboratories, Mexico). LA sodium salt with a purity of 99% and tetramethylrhodamine (TRITC)-conjugated phalloidin were from Sigma-Aldrich (Merck KGaA). Anti-vimentin antibody (Ab), anti-E-cadherin Ab and anti-focal adhesion kinase (FAK) Ab were from Santa Cruz Biotechnology (Sta. Cruz, CA, USA). Anti-paxillin Ab was from Abcam® (Waltham, MA, USA). Phospho-specific Ab to tyrosine (Tyr)-397 of FAK (anti-FAK-p-Tyr397) was from Invitrogen (Camarillo, CA, USA). Anti-actin Ab was from R&D Systems, Inc (Minneapolis, MN, USA)

Cell lines and culture

MDA-MB-231 and MCF-7 breast cancer cells were cultured in Dulbecco's modified Eagle's medium (DMEM) supplemented with 5% fetal bovine serum (FBS), 3.7 g/l sodium bicarbonate and antibiotics. Cultures were incubated under a humidified atmosphere containing 5% CO_2 and 95% air at 37 ºC. MDA-MB-231 cells were FBS-starved in DMEM for 24 h and MCF-7 cells were FBS-starved in DMEM for 18 h before treatment with BLf, FBS and/or LA.

Cell stimulation

Cultures of MDA-MB-231 and MCF-7 cells were washed twice with phosphate-buffered saline (PBS), equilibrated in DMEM for 30 min and treated for various times and concentrations of Apo-BLf, Holo-BLf, FBS or LA. After stimulation, conditioned media were collected and cells were solubilized in 0.5 ml ice-cold RIPA buffer (50 mM HEPES pH 7.4, 150 mM NaCl, 1 mM EGTA, 1 mM sodium orthovanadate, 100

mM NaF, 10 mM sodium pyrophosphate, 10% glycerol, 1% Triton X100, 1% sodium deoxycholate, 1.5 mM $MgCl_2$, 0.1% SDS and 1 mM PMSF). Protein concentration of samples was determined by the micro-Bradford protein assay (Bio-Rad, USA).

Western blot (WB) analysis

Equal amounts of protein were separated using 10% SDS-PAGE separating gels followed by transfer to nitrocellulose membranes. Membranes were blocked for 2 h at room temperature using 5% non-fat dried milk in PBS pH 7.2/0.1% Tween 20 (wash buffer), and incubated overnight at 4 ºC with primary Ab. Membranes were washed three times with wash buffer and incubated with secondary Ab conjugated to horseradish peroxidase for 2 h at room temperature. After washing three times with wash buffer, immunoreactive bands were visualized using WB luminol reagent and exposition to an autoradiography film. For quantification, autoradiograms were scanned and bands were analyzed using the ImageJ software v. 1.52e (NIH, USA).

Scratch-wound assay

Cultures were treated for 2 h with 12 µM mitomycin C to inhibit proliferation during the experiment. Cell cultures were scratched, washed twice with PBS and supplemented with FBS-free DMEM with or without BLf, FBS and LA for 48 h at 37 ºC. Cultures were photographed using an inverted microscope coupled to a camera. Images from ≥ 3 fields per experimental condition were acquired and analyzed using the ImageJ software v. 1.52e (NIH, USA).

Invasion assays

Inserts of 24-well plates were covered with 30 ml Matrigel (3 mg/ml) and incubated overnight at 37 ºC. Next, MDA-MB-231 cells (1×10^5) were plated on Matrigel of each insert (Upper chamber) in fresh FBS-free DMEM. Lower chamber contained 600 ml FBS-free DMEM without or with Holo-BLf. Plates were incubated for 48 h at 37 °C under a humidified atmosphere with 5% CO_2 and 95% air. After incubation, cells and Matrigel on the upper surface of membranes were removed with cotton swabs, and the cells on the lower surface of membranes were washed with PBS and fixed with methanol for 5 min at room temperature. Quantification of invaded cells was determined by staining of membranes with crystal violet (0.5%) in PBS for 15 min at room temperature and elution of dye with 300 ml acetic acid (10%). Absorbance of collected solution was measured at 600 nm.

Zymography

Conditioned media were concentrated using 5,000 Da Centricon® filters (EDM Millipore). Equal volumes of non-heated conditioned medium and sampler buffer (2.5% SDS, 2% sucrose, 4 µg/ml phenol red) were mixed and loaded into 8% polyacrylamide gels copolymerized with gelatin (1 mg/ml). After electrophoresis at 72 V for 2 h, gels were rinsed twice for 30 min with 2.5% Triton X-100, and incubated in assay buffer (50 mM Tris–HCl pH 7.4, 5 mM $CaCl_2$) at 37 °C for 48 h. Gels were fixed and stained with a

solution of Coomassie Brilliant Blue G-250 (0.25%) dissolved in acetic acid (10%) and methanol (30%). Proteolytic activity was identified as clear bands against the background stain of undigested substrate in the gel. Controls of MMP-2 and MMP-9 secretions were included, which were prepared by treatment of MDA-MB-231 cells with 400 mg/dl ethanol and 100 ng/ml PDB for 24 h at 37 ºC respectively [19, 20].

Immunofluorescence confocal microscopy

MDA-MB-231 cells were grown on coverslips, washed with PBS, equilibrated in FBS-free DMEM and treated with Holo-BLf and/or FBS for 20 min at 37 °C. Cells were fixed with paraformaldehyde (4%) for 20 min, permeabilized with 0.5% Triton X-100 for 20 min and blocked with blocking solution (0.5% gelatin, 1 mM $CaCl_2$, 0.5 mM $MgCl_2$ in PBS) for 20 min at room temperature. Cells were incubated for 12 h at 4 °C with anti-paxillin Ab (1:1000) followed by FITC-labeled anti-mouse secondary Ab for 2 h at room temperature. Staining of fibrillar actin was performed by incubation of cells for 2 h at room temperature with TRITC-conjugated phalloidin. Cells were mounted on glass slides using Vectashield and analyzed by confocal microscopy (Model TCS SP2; Leica Microsystems, Inc). Images were analyzed by using the ImageJ software v. 1.52e (NIH, USA).

Statistical analysis

Data are expressed as mean ± SD of at least three independent experiments, and were analyzed using one-way ANOVA and Dunnett's multiple comparison test. Statistical probability of $P<0.05$ was considered significant.

Results

BLf does not induce migration in MDA-MB-231 breast cancer cells

We determined whether Holo-BLf and Apo-BLf induced migration in MDA-MB-231 breast cancer cells. Migration assays were performed using scratch-wound assays with MDA-MB-231 cells treated with increasing concentrations of Holo-BLf and Apo-BLf for 48h. Findings showed that treatment with Holo-BLf and Apo-BLf did not induce migration in MDA-MB-231 breast cancer cells (Fig. 1A and B).

BLf inhibits migration induced by FBS

We determined whether Holo-BLf and Apo-BLf inhibited the migration induced by stimulation with FBS. Migration assays were performed using scratch-wound assays with MDA-MB-231 cells cotreated with 5% FBS and increasing concentrations of Holo-BLf or Apo-BLf. Findings showed that treatment with Holo-BLf and Apo-BLf partly inhibited the migration induced by FBS in MDA-MB-231 cells. Particularly, treatment with 2500 nM Holo-BLf inhibited migration by ~ 90%, whereas 2500 nM Apo-BLf inhibited migration by ~ 50% induced by FBS in MDA-MB-231 cells (Fig. 2A and B).

BLf inhibits migration induced by LA

LA induces migration and invasion in MDA-MB-231 cells [21, 22]. We determined whether Holo-BLf and Apo-BLf inhibited migration induced by LA. Migration assays were performed using scratch-wound assays with MDA-MB-231 cells cotreated with increasing concentrations of Holo-BLf or Apo-BLf and 90 μM LA for 48 h. Findings demonstrated that treatment with 125 nM and 1250 nM Holo-BLf inhibited migration by 90% and to basal levels with 2500 nM Holo-BLf, whereas treatment with 1250 nM and 2500 nM Apo-BLf inhibited by 50% migration induce by LA in MDA-MB-231 cells (Fig. 3A and B).

BLf inhibits invasion induced by FBS

Since Holo-BLf inhibited migration to basal levels, we determined whether Holo-BLf inhibited invasion and secretion of MMP-2 and MMP-9 induced by FBS. Invasion assays were performed with MDA-MB-231 cells cotreated with 2500 nM Holo-BLf and FBS. Findings demonstrated that treatment with Holo-BLf partly inhibited invasion induced by FBS (Fig. 4A).

To determine whether Holo-BLf induced inhibition of MMP-2 and MMP-9 secretion induced by FBS, MDA-MB-231 cells were cotreated with 2500 nM Holo-BLf and FBS, and then conditioned media were obtained. MMP-2 and MMP-9 secretions were analyzed by gelatin zymography of conditioned media. Findings showed that treatment with Holo-BLf partly inhibited MMP-2 and MMP-9 secretion induced by FBS (Fig. 4B).

Next, we determined whether Holo-BLf induced regulation in the expression of the epithelial protein E-cadherin and the mesenchymal protein vimentin. MDA-MB-231 and MCF-7 breast cancer cells were treated with 125 nM and 1250 nM Holo-BLf for 24 h and cells were lysed. Cell lysates were analyzed by WB with anti-E-cadherin Ab and anti-vimentin Ab. Findings showed that Holo-BLf did not induce downregulation of E-cadherin expression in MCF-7 cells, and it did not induce E-cadherin expression in MDA-MB-231 cells. In contrast, 1250 nM Holo-BLf induced downregulation of vimentin expression in MCF-7 cells and 1250 nM Holo-BLf induced inhibition of vimentin expression in MDA-MB-231 cells (Fig. 4C).

BLf promotes the formation of focal adhesions

We studied whether Holo-BLf regulated FAK activation induced by FBS. MDA-MB-231 cells were treated for 1 h with 1250 nM Holo-BLf and then cells were stimulated with 5% FBS for 60 min and lysed. FAK activation was analyzed by WB of cell lysates with anti-FAK-p-Tyr397 Ab. Results demonstrated that Holo-BLf partly inhibited FAK phosphorylation at Tyr-397 and then its activation induced by FBS in MDA-MB-231 cells (Fig 5A).

Next, we determined whether Holo-BLf regulated the formation of focal adhesions. MDA-MB-231 cells were cultured on coverslips and treated for 1 h with 1250 nM Holo-BLf and then cells were stimulated with 5% FBS for 20 min. Focal adhesions were analyzed by immunofluorescence analysis of paxillin, because it is a protein localized in focal adhesions [23]. Findings showed that Holo-BLf induced the assembly of some focal adhesions, whereas FBS induced a high increase in the assembly and then

number of focal adhesions in MDA-MB-231 cells. Interestingly, treatment with Holo-BLf increased the number and size of focal adhesions induced by FBS in MDA-MB-231 cells (Fig. 5B).

Discussion

In adenocarcinomas, metastasis is the dissemination of cancer cells from primary tumors to distant organs, and it requires the migration and invasion of cancer cells into adjacent tissues and the intravasation into blood and/or lymphatic vessels [24, 25]. Moreover, BLf (1 μM) enhances migration of WI-38 human fetal fibroblasts, whereas recombinant human Lf (50–200 μg/ml) induces migration of human dermal fibroblasts [26, 27]. In contrast to these findings, we demonstrate that Holo-BLf and Apo-BLf do not induce migration in MDA-MB-231 breast cancer cells. Since, human fetal fibroblasts WI-38 and human dermal fibroblasts are not cancerous cells, we propose that BLf induces migration in non-cancer cells but it does not induce migration in breast cancer cells.

It has been suggested an association between high levels of dietary fat intake and an increased risk of developing breast cancer [28, 29]. LA is an omega-6 essential fatty acid and the major polyunsaturated fatty acid in most diets, which contributes to the development of chronic diseases [30]. In MDA-MB-231 breast cancer cells, LA induces FAK activation, migration and invasion through a FFAR4- and PI3K-/Akt-dependent pathway [21, 22]. We demonstrate that treatment with 2500 nM Holo-BLf inhibit completely the migration induced by LA, whereas treatment with 2500 nM Holo-BLf inhibit by ∼90% the migration induced by FBS in MDA-MB-231 cells. In contrast, treatment with 2500 nM Apo-BLf inhibit by ∼ 50% the migration induced by LA and FBS in MDA-MB-231 cells. Since, Apo-BLf and Holo-BLf present a different three-dimensional conformation depending on its binding to Fe^{3+} [5], our results demonstrate that Holo-BLf conformation has a bigger capacity for inhibition of migration induced by FBS and LA than Apo-BLf conformation in MDA-MB-231 breast cancer cells. In contrast, it has been demonstrated that treatment with 10 nM Apo-BLf has a bigger capacity for inhibition of migration induced by FBS than Holo-BLf in MDA-MB-231 and MCF-7 breast cancer cells [31]. We propose that Apo-BLf and Holo-BLf and their different concentrations used in the different studies show different capacities of inhibition of specific cell processes in breast cancer cells, including the migration induced by FBS. Supporting our proposal, Holo-BLf has a bigger capacity for inhibition of proliferation induced by FBS than Apo-BLf in MDA-MB-231 cells, however Holo-BLf and Apo-BLf show a similar capacity of inhibition of proliferation induce by FBS in MCF-7 cells [31]. Moreover, Apo-BLf is more effective at inducing cell cytotoxicity than Holo-BLf in MDA-MB-231 and MCF-7 cells [31].

Epithelial to mesenchymal transition (EMT) is the transdifferentiation of epithelial cells to a mesenchymal type, which has been implicated in tumor progression, because epithelial cells acquire the capacity to execute the steps of invasion and metastasis [32]. Particularly, EMT process involves the loss of apico-basal polarity, dismantling of adherens junctions and the expression of mesenchymal markers including vimentin, N-cadherin, α-smooth muscle actin, myosin isoforms, fibronectin and FSP-1, and the loss of epithelial characteristics, including downregulation of E-cadherin expression [32, 33]. We demonstrate that Holo-BLf induces downregulation of vimentin expression in MDA-MB-231 and MCF-7

cells. In addition, Holo-BLf does not induce downregulation of E-cadherin expression in MCF-7 cells, and it does not induce E-cadherin expression in MDA-MB-231 cells. We propose that Holo-BLf might inhibit the expression of mesenchymal markers and the downregulation of epithelial markers and then inhibit the EMT process in breast cancer cells. Supporting our proposal, Holo-BLf induces a higher inhibition of vimentin expression than Apo-BLf in human glioblastoma GL-15 cells, whereas high concentrations of BLf (10 and 100 µg/ml) induces upregulation of E-cadherin expression and downregulation of vimentin expression in malignant oral squamous carcinoma cells HOC3313 [34, 35].

Hallmark of EMT is the acquisition of the capacity to migrate and invade the extracellular matrix, which require the activation of signal transduction pathways that mediate a variety of specific cell processes, including focal adhesion assembly and the secretion of certain MMPs, such as gelatinases (MMP-2 and MMP-9) [33]. We demonstrate that Holo-BLf partly inhibits invasion and MMP-2 and MMP-9 secretion induced by FBS in MDA-MB-231 cells. In agreement with our findings, BLf partly inhibits invasion in HOC3313 and SCCVII oral squamous carcinoma cells [34]. Our findings support the proposal that Holo-BLf partly inhibits the EMT process in breast cancer cells.

Focal adhesions are structures wherein integrin receptors mediate the interaction between the actin cytoskeleton and extracellular matrix, which are composed of diverse cell components including scaffolding proteins, adaptor proteins, GTPases, phosphatases and kinases, such as FAK and Src [36, 37]. FAK is a 125 kDa protein tyrosine kinase that is activated by a variety of agonists and is implicated in the regulation of cell spreading, differentiation, proliferation, migration, invasion survival and angiogenesis [38, 39]. FAK is activated by its phosphorylation at Tyr-397, which creates a binding site for SH2 domains of several proteins including Src family kinases. FAK/Src complex mediates the assembly and disassembly of focal adhesions, which regulate cell migration and invasion, and then they have been implicated in the EMT process [38, 40, 41]. We demonstrate that Holo-BLf induce an increase in FAK phosphorylation at Tyr-397 and its activation, and an increase in the number and size of focal adhesions induced by FBS in MDA-MB-231 cells. In agreement with our findings, a peptide corresponding to residues 17–41 near the N-terminus of BLf induces FAK and paxillin tyrosine phosphorylation in intestinal epithelial cells IEC-6 [42]. We propose that Holo-BLf induces inhibition of migration and invasion via the inhibition of phosphatases that dephosphorylate FAK and the inhibition of proteins that mediate the disassembly of focal contacts. Our finding support the proposal that Holo-BLf inhibits the EMT process in breast cancer cells.

In conclusion, our findings demonstrate that Holo-BLf inhibits cellular processes involved with the migration and invasion process in breast cancer cells. We propose that Holo-BLf inhibit the EMT process in breast cancer cells.

Declarations

Acknowledgments

We are grateful to Nora Ruiz for her technical assistance.

Author contributions

N R-O, K R-R: design, conduction, data analysis, methodology, validation and manuscript preparation. P C-R, MG, EPS: Conceptualization, Methodology, Writing-Review and editing, Project administration, Funding acquisition, Visualization, Supervision

Funding

This research was funded by CONACYT (255429), Mexico. Grants from CONACYT supported N R-O and K R-R.

Ethical approval

This article does not contain any studies with human participants or animals performed by any of the authors.

Conflict of interest

The authors declare that they have no conflicts of interests

References

1. Bray F, Ferlay J, Soerjomataram I, Siegel RL, Torre LA, Jemal A (2018) Global cancer statistics 2018: GLOBOCAN estimates of incidence and mortality worldwide for 36 cancers in 185 countries. CA Cancer J Clin 68:394–424
2. Albuquerque RC, Baltar VT, Marchioni DM (2014) Breast cancer and dietary patterns: a systematic review. Nutr Rev 72:1–17
3. Harbeck N, Penault-Llorca F, Cortes J, Gnant M, Houssami N, Poortmans P, Ruddy K, Tsang J, Cardoso F (2019) Breast cancer. Nat Rev Dis Primers 5:66
4. Chajes V, Romieu I (2014) Nutrition and breast cancer. Maturitas 77:7–11
5. Gonzalez-Chavez SA, Arevalo-Gallegos S, Rascon-Cruz Q (2009) Lactoferrin: structure, function and applications. Int J Antimicrob Agents 33:301e301–301e308
6. van der Strate BW, Beljaars L, Molema G, Harmsen MC, Meijer DK (2001) Antiviral activities of lactoferrin. Antiviral Res 52:225–239
7. Alexander DB, Iigo M, Yamauchi K, Suzui M, Tsuda H (2012) Lactoferrin: an alternative view of its role in human biological fluids. Biochem Cell Biol 90:279–306
8. Schanbacher FL, Goodman RE, Talhouk RS (1993) Bovine mammary lactoferrin: implications from messenger ribonucleic acid (mRNA) sequence and regulation contrary to other milk proteins. J Dairy Sci 76:3812–3831
9. Conneely OM (2001) Antiinflammatory activities of lactoferrin. J Am Coll Nutr 20:389S–395S discussion 396S-397S

10. Hao L, Shan Q, Wei J, Ma F, Sun P (2019) Lactoferrin: Major Physiological Functions and Applications. Curr Protein Pept Sci 20:139–144
11. Gruden S, Poklar Ulrih N (2021) Diverse Mechanisms of Antimicrobial Activities of Lactoferrins, Lactoferricins, and Other Lactoferrin-Derived Peptides.Int J Mol Sci22
12. Cutone A, Rosa L, Ianiro G, Lepanto MS, Bonaccorsi di Patti MC, Valenti P, Musci G (2020) Lactoferrin's Anti-Cancer Properties: Safety, Selectivity, and Wide Range of Action. Biomolecules 10
13. Iigo M, Alexander DB, Long N, Xu J, Fukamachi K, Futakuchi M, Takase M, Tsuda H (2009) Anticarcinogenesis pathways activated by bovine lactoferrin in the murine small intestine. Biochimie 91:86–101
14. Tsuda H, Sekine K, Fujita K, Ligo M (2002) Cancer prevention by bovine lactoferrin and underlying mechanisms–a review of experimental and clinical studies. Biochem Cell Biol 80:131–136
15. Xu XX, Jiang HR, Li HB, Zhang TN, Zhou Q, Liu N (2010) Apoptosis of stomach cancer cell SGC-7901 and regulation of Akt signaling way induced by bovine lactoferrin. J Dairy Sci 93:2344–2350
16. Damiens E, El Yazidi I, Mazurier J, Duthille I, Spik G, Boilly-Marer Y (1999) Lactoferrin inhibits G1 cyclin-dependent kinases during growth arrest of human breast carcinoma cells. J Cell Biochem 74:486–498
17. Duarte DC, Nicolau A, Teixeira JA, Rodrigues LR (2011) The effect of bovine milk lactoferrin on human breast cancer cell lines. J Dairy Sci 94:66–76
18. Avalos-Gomez C, Reyes-Lopez M, Ramirez-Rico G, Diaz-Aparicio E, Zenteno E, Gonzalez-Ruiz C, de la Garza M (2020) Effect of apo-lactoferrin on leukotoxin and outer membrane vesicles of Mannheimia haemolytica A2. Vet Res 51:36
19. Ke Z, Lin H, Fan Z, Cai TQ, Kaplan RA, Ma C, Bower KA, Shi X, Luo J (2006) MMP-2 mediates ethanol-induced invasion of mammary epithelial cells over-expressing ErbB2. Int J Cancer 119:8–16
20. Park MJ, Park IC, Hur JH, Rhee CH, Choe TB, Yi DH, Hong SI, Lee SH (2000) Protein kinase C activation by phorbol ester increases in vitro invasion through regulation of matrix metalloproteinases/tissue inhibitors of metalloproteinases system in D54 human glioblastoma cells. Neurosci Lett 290:201–204
21. Serna-Marquez N, Diaz-Aragon R, Reyes-Uribe E, Cortes-Reynosa P, Salazar EP (2017) Linoleic acid induces migration and invasion through FFAR4- and PI3K-/Akt-dependent pathway in MDA-MB-231 breast cancer cells. Med Oncol 34:111
22. Serna-Marquez N, Villegas-Comonfort S, Galindo-Hernandez O, Navarro-Tito N, Millan A, Salazar EP (2013) Role of LOXs and COX-2 on FAK activation and cell migration induced by linoleic acid in MDA-MB-231 breast cancer cells. Cell Oncol (Dordr) 36:65–77
23. Schaller MD (2001) Paxillin: a focal adhesion-associated adaptor protein. Oncogene 20:6459–6472
24. Chambers AF, Groom AC, MacDonald IC (2002) Dissemination and growth of cancer cells in metastatic sites. Nat Rev Cancer 2:563–572

25. Friedl P, Wolf K (2003) Tumour-cell invasion and migration: diversity and escape mechanisms. Nat Rev Cancer 3:362–374
26. Tang L, Cui T, Wu JJ, Liu-Mares W, Huang N, Li J (2010) A rice-derived recombinant human lactoferrin stimulates fibroblast proliferation, migration, and sustains cell survival. Wound Repair Regen 18:123–131
27. Takayama Y, Mizumachi K (2001) Effects of lactoferrin on collagen gel contractile activity and myosin light chain phosphorylation in human fibroblasts. FEBS Lett 508:111–116
28. Fay MP, Freedman LS, Clifford CK, Midthune DN (1997) Effect of different types and amounts of fat on the development of mammary tumors in rodents: a review. Cancer Res 57:3979–3988
29. Lee MM, Lin SS (2000) Dietary fat and breast cancer. Annu Rev Nutr 20:221–248
30. Simopoulos AP (2006) Evolutionary aspects of diet, the omega-6/omega-3 ratio and genetic variation: nutritional implications for chronic diseases. Biomed Pharmacother 60:502–507
31. Gibbons JA, Kanwar JR, Kanwar RK (2015) Iron-free and iron-saturated bovine lactoferrin inhibit survivin expression and differentially modulate apoptosis in breast cancer. BMC Cancer 15:425
32. Thiery JP (2003) Epithelial-mesenchymal transitions in development and pathologies. Curr Opin Cell Biol 15:740–746
33. Thiery JP, Sleeman JP (2006) Complex networks orchestrate epithelial-mesenchymal transitions. Nat Rev Mol Cell Biol 7:131–142
34. Chea C, Miyauchi M, Inubushi T, Okamoto K, Haing S, Nguyen PT, Imanaka H, Takata T (2018) Bovine lactoferrin reverses programming of epithelial-to-mesenchymal transition to mesenchymal-to-epithelial transition in oral squamous cell carcinoma. Biochem Biophys Res Commun 507:142–147
35. Cutone A, Colella B, Pagliaro A, Rosa L, Lepanto MS, Bonaccorsi di Patti MC, Valenti P, Di Bartolomeo S, Musci G (2020) Native and iron-saturated bovine lactoferrin differently hinder migration in a model of human glioblastoma by reverting epithelial-to-mesenchymal transition-like process and inhibiting interleukin-6/STAT3 axis. Cell Signal 65:109461
36. Guo W, Giancotti FG (2004) Integrin signalling during tumour progression. Nat Rev Mol Cell Biol 5:816–826
37. Wozniak MA, Modzelewska K, Kwong L, Keely PJ (2004) Focal adhesion regulation of cell behavior. Biochim Biophys Acta 1692:103–119
38. Parsons JT (2003) Focal adhesion kinase: the first ten years. J Cell Sci 116:1409–1416
39. Zhao J, Guan JL (2009) Signal transduction by focal adhesion kinase in cancer. Cancer Metastasis Rev 28:35–49
40. Webb DJ, Donais K, Whitmore LA, Thomas SM, Turner CE, Parsons JT, Horwitz AF (2004) FAK-Src signalling through paxillin, ERK and MLCK regulates adhesion disassembly. Nat Cell Biol 6:154–161
41. Avizienyte E, Frame MC (2005) Src and FAK signalling controls adhesion fate and the epithelial-to-mesenchymal transition. Curr Opin Cell Biol 17:542–547

42. Jeong YY, Lee GY, Yoo YC (2021) Bovine Lactoferricin Induces Intestinal Epithelial Cell Activation through Phosphorylation of FAK and Paxillin and Prevents Rotavirus Infection. J Microbiol Biotechnol 31:1175–1182

Figures

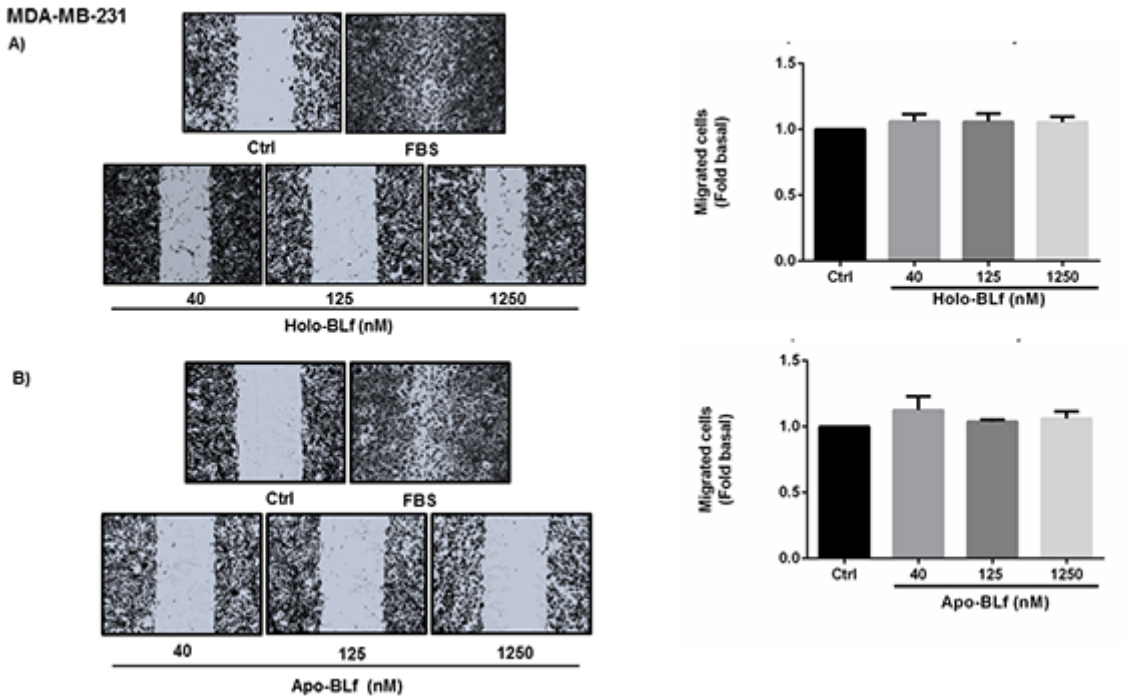

Figure 1

BLf does not induce migration in MDA-MB-231 breast cancer cells

a and b Migration assays were performed with MDA-MB-231 cells treated with increasing concentration of Holo-BLf and Apo-BLf. One control of cell migration was included (FBS). Graphs represent the mean ±S.D. and indicate the fold of migration above control (Ctrl) value (unstimulated cells).

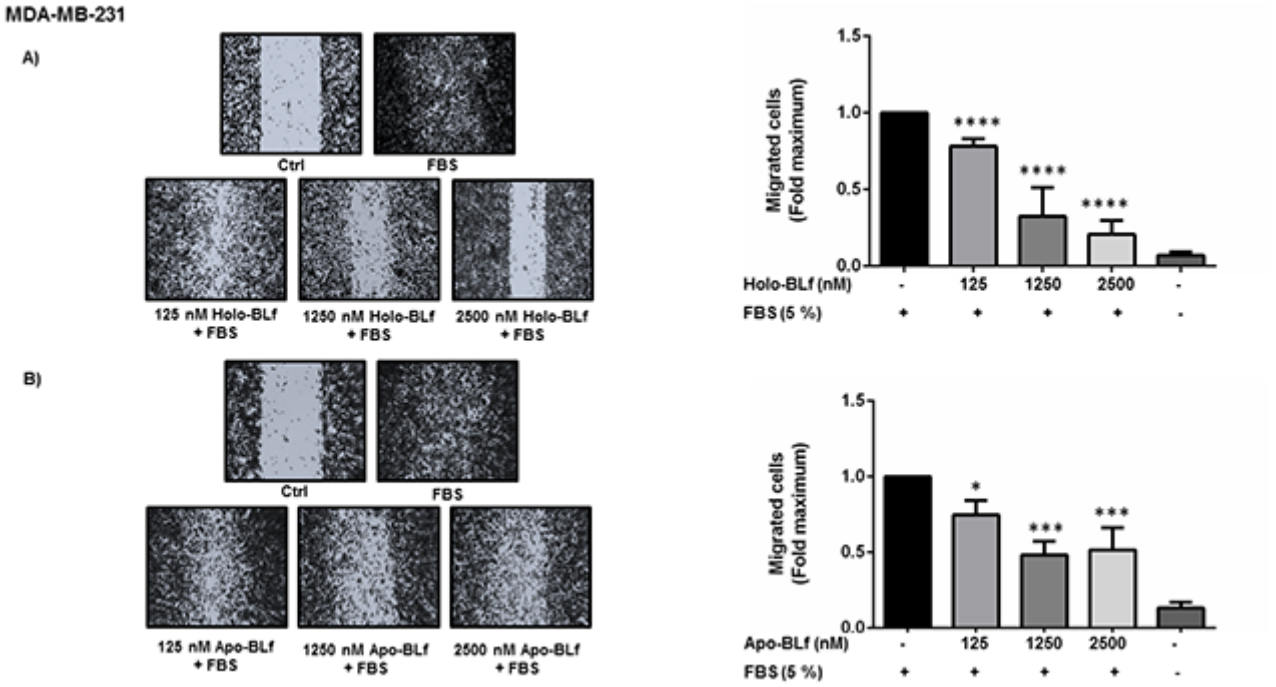

Figure 2

BLf inhibits migration induced by FBS

a and b Migration assays were performed with MDA-MB-231 cells cotreated with increasing concentrations of Holo-BLf and Apo-BLf and 5 % FBS. One control of cell migration was included (FBS). Graphs represent the mean ±S.D. and indicate the fold of migration above Ctrl value. **P<0.05, ***P<0.001, ****P<0.0001*

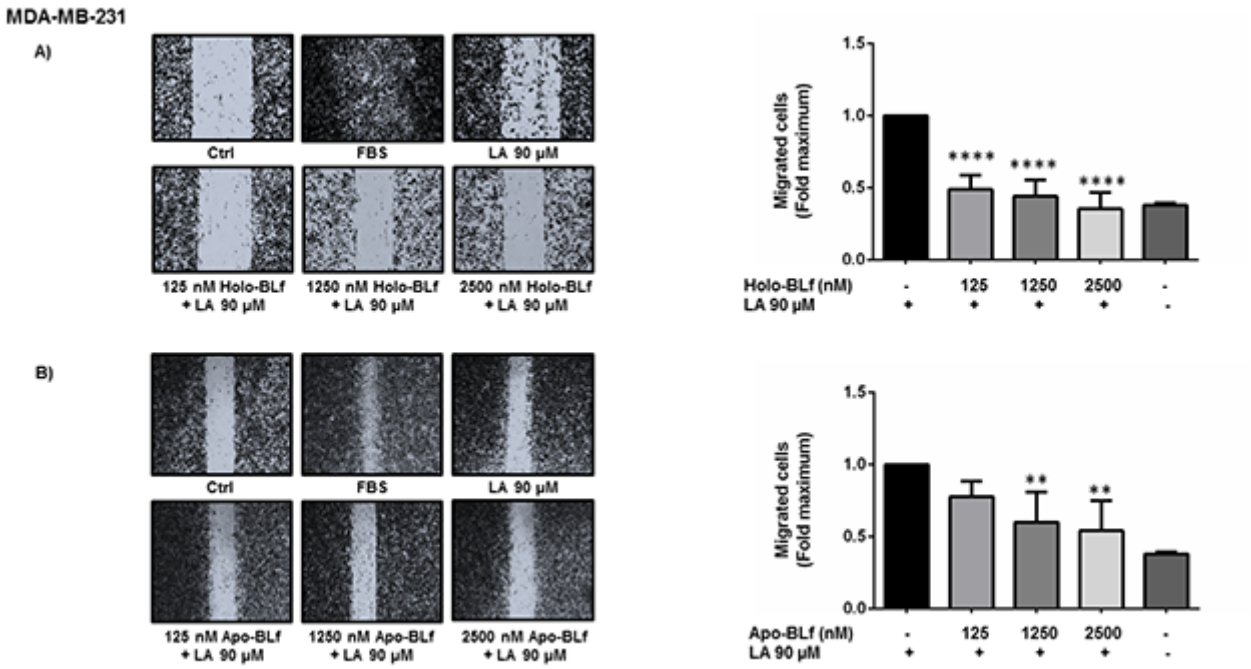

Figure 3

BLf inhibits migration induced by LA

a and b Migration assays were performed with MDA-MB-231 cells cotreated with increasing concentrations of Holo-BLf and Apo-BLf and 90 µM LA. One control of cell migration was included (FBS). Graphs represent the mean ±S.D. and indicate the fold of migration above Ctrl value. ***P<0.01. ****P<0.0001*

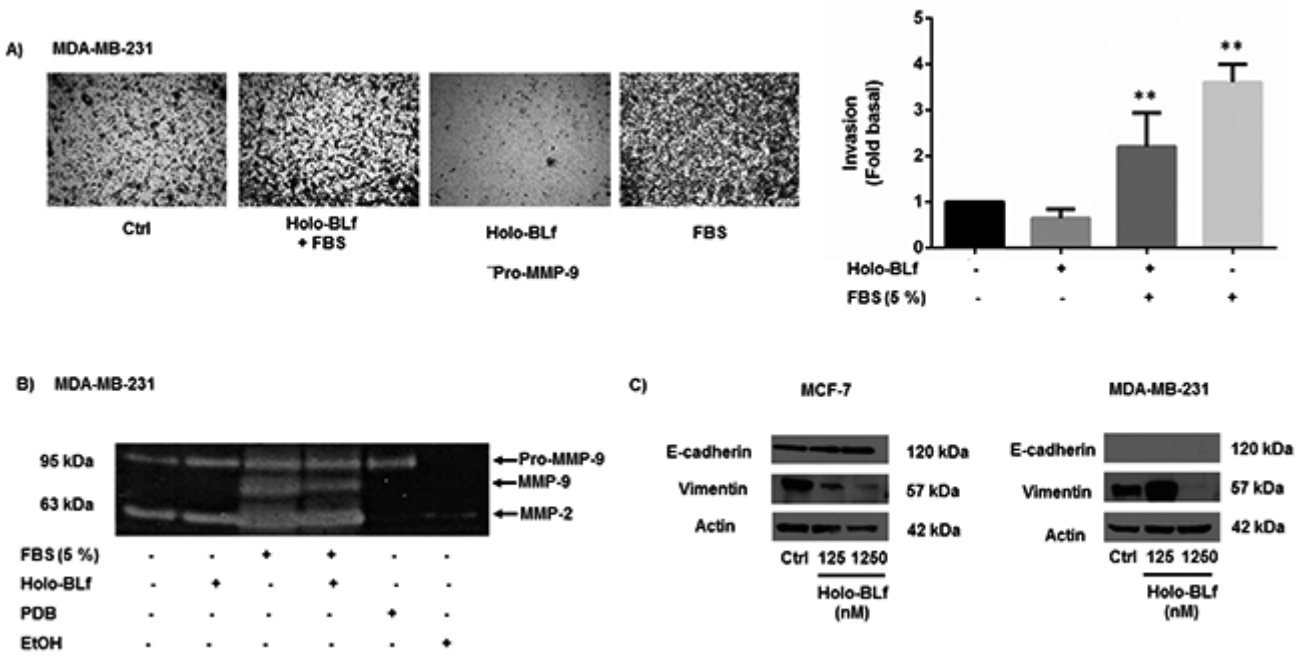

Figure 4

BLf inhibits invasion and expression of mesenchymal proteins

a Invasion assays were performed with MDA-MB-231 cells cotreated with 2500 nM Holo-BLf and 5% FBS. One control of invasion was included (FBS). **b** MDA-MB-231 cells were cotreated with 2500 nM Holo-BLf and 5% FBS for 48 h and then conditioned media were obtained. MMP-2 and MMP-9 secretion was analyzed by gelatin-substrate gels. Positive controls of MMP-2 (EtOH) and MMP-9 (PDB) secretion were included. **c** Cell lysates from MDA-MB-231 and MCF-7 cells treated with 125 nM and 1250 nM Holo-BLf for 24 h were analyzed by WB with anti-E-cadherin Ab, anti-vimentin Ab and anti-actin Ab. Graph represents the mean ±S.D. and indicate the fold of invasion above Ctrl value. ***P<0.01*

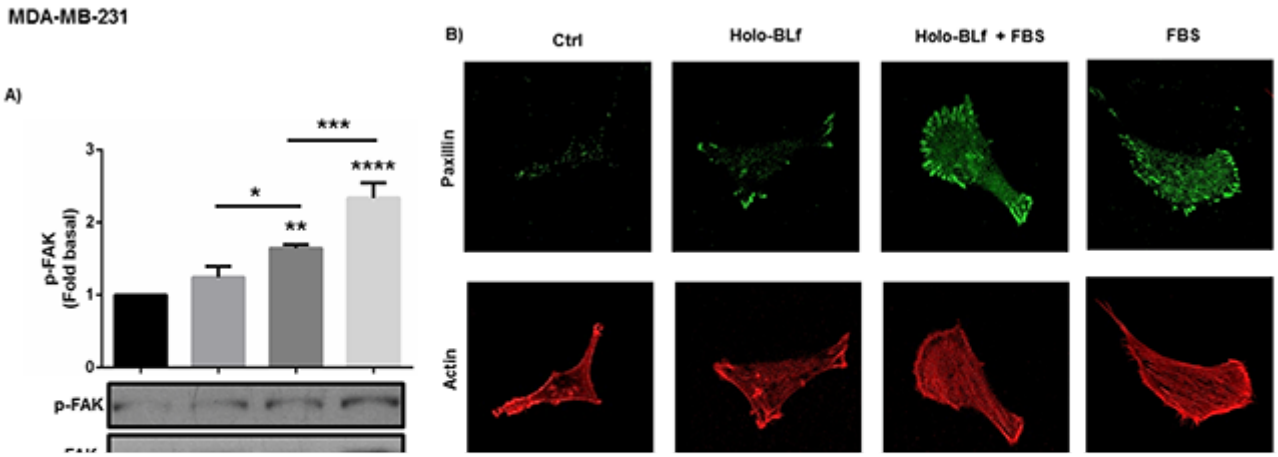

Figure 5

BLf inhibits FAK activation and induces formation of focal contacts

a Cell lysates from MDA-MB-231 cells cotreated with 2500 nM Holo-BLf and 5% FBS for 40 min were analyzed by WB with anti-FAK-p-Tyr397 Ab, anti-FAK Ab and anti-actin Ab. **b** MDA-MB-231 cells cultured on coverslips were cotreated with 2500 nM Holo-BLf and 5% FBS for 40 min. Cells were fixed and analyzed by staining with anti-paxillin Ab conjugated to FITC. F-actin was stained with TRITC-conjugated phalloidin. F-actin structures are shown in red, and focal contacts are shown in green. Graph represents the mean ±S.D. and indicates FAK phosphorylated at Tyr397 (p-FAk) above Ctrl value. **P<0.05, **P<0.01, ***P<0.001, ****P<0.0001*